Arch. Metall. Mater. **67** (2022), 2, 547-554

DOI: https://doi.org/10.24425/amm.2022.137789

L. BENEA[1]

THE CONTRIBUTION OF ELECTROCHEMISTRY FOR A BETTER UNDERSTANDING OF THE DEGRADATION BY TRIBOCORROSION OF METALLIC IMPLANT MATERIALS

In this paper there are presented some results obtained by open circuit potential and electrochemical impedance spectroscopy measurements from studies performed on the behavior of tribocorrosion on metallic implant biomaterials as: 304L stainless steel, Co/nano-CeO_2 nanocomposite layer and Ti6Al4V untreated and oxidized alloy to form a nanoporous TiO_2 film. The open circuit potential technique used in measuring the tribocorrosion process provide information on the active or passive behavior of the investigated metallic biomaterial in the biological fluid, before, during friction and after stopping the friction. Thus it clearly show a better behavior of Co/nano-CeO_2 nanocomposite coatings as compared with 304L stainless steel to tribocorrosion degradation in Hank solution; as well the better behavior of nanoporous TiO_2 film formed annodically on Ti6Al4V alloy surface as compared with untreated alloy to tribocorrosion degradation in artificial saliva Fusayama Meyer. The slight decrease in polarization resistance value resulted from electrochemical impedance spectroscopy measured during friction in the case of the Co/nano-CeO_2 nanocomposite layer (four times smaller), compared to 304L stainless steel, whose polarization resistance decreased more than 1000 times during friction shows the higher sensitivity of stainless steel to degradation by tribocorrosion. The same behavior is observed when comparing the polarization resistance of untreated titanium alloy recorded during friction that is about 200 hundred times smaller, while the specific polarization resistance of the oxidized alloy with the nanoporous film of titanium oxide, decreases very little during friction, highlighting the beneficial effect of modifying the titanium alloy by anodic oxidation to increase its resistance to the degradation process by tribocorrosion.

Keywords: Tribocorrosion; Biological fluids; Biomaterials; Nano composite layer; Electrochemical methods

1. Introduction

The tribocorrosion can be defined as the degradation process, which takes place under the combined action of friction and corrosion in an aggressive corrosive environment. In practice, tribocorrosion can affect a large number of very diverse tribological systems, made up of mechanical devices comprising generally metallic parts in contact and in relative movement (pump mechanisms, bearings, gears, hinges, orthopedic implants, etc.) placed in an environment proving corrosive for the metallic materials constituting the tribological surfaces. It is important to note that due to the joint mechanisms of friction and corrosion reasoning based solely on the hardness or other physical characteristics of a material will not predict the life of any particular material involved in a contact [1-6].

Tribocorrosion phenomena can influence a large number of industrial areas ranging from the transport sector to the energy sector, areas of strategic importance, as well as the biomedical applications [7-17]. Tribocorrosion degradation can take place on different parts of medical devices such as hip implants, dental implants and fracture fixation devices.

In recent years, we find in the literature the growing interest in the use of electrochemical techniques for the study of the mechanism of tribocorrosion process [1-8].

The influence of the electrochemical state of the surface of a material (active, passive) has been studied by different authors [1,2,6], as well as the influence of friction on the free potential [4,7] or the influence of friction on the electrochemical impedance spectroscopy [9,11]. These electrochemical techniques have also been used to quantify the synergic effect between friction and corrosion [2,4].

Tribocorrosion finds applications in almost all areas of biomedical implants as the interaction of biomedical chemicals on implants, evaluation of degradation of arch-wire or dental implants. The functionality of a surface is often at the heart of the success or otherwise of engineering systems.

[1] DUNAREA DE JOS UNIVERSITY OF GALATI, FACULTY OF ENGINEERING, COMPETENCES CENTRE: INTERFACES-TRIBOCORROSION-ELECTROCHEMICAL SYSTEMS (CC-ITES), 47 DOMNEASCA STREET, RO-800008 GALATI, ROMANIA

* Coressponding author: lidia.benea@ugal.ro

Therefore, the electrochemical techniques such as open circuit potential and electrochemical impedance spectroscopy measurements are essential tools for the degradation study of the metallic implant materials by tribocorrosion process. In this paper are presented some representative results obtained by open circuit potential and electrochemical impedance spectroscopy measurements from studies performed on the behavior of stainless steel, Co/nano-CeO_2 and untreated and oxidized titanium alloy to tribocorrosion degradation in biological fluids.

2. Experimental

The tribocorrosion process refers to the science of surface transformations, which results from the interaction of mechanical and chemical processes that take place between the elements of a tribosystem exposed to corrosive environments. Thus, this process combines mechanical and chemical interactions between two surfaces and the environment, including processes of friction, lubrication, wear and chemical and electrochemical reactions.

Tribocorrosion is an irreversible process of material transformation, which involves many synergic effects of a chemical, mechanical and / or electrochemical nature and occurs when sliding, rolling, erosion or abrasion are present. This synergism in materials degradation is often much greater or less than would be expected from a simple summation of mechanical and environmental effects [17].

Two principal approaches are used in the laboratory in order to study the biomaterials behavior to tribocorrosion degradations in biological fluids. One is pin on disc sliding unidirectional fretting as it can be seen in Fig. 1a and the other one is bidirectional fretting, schematically represented in Fig. 1b. In both experimental set-up, the materials to be studied is mounted in a three electrodes electrochemical cell as the working electrode (WE). The counter electrode is an inert electrode as platinum and the reference electrode most usual being silver-silver chloride electrode, Ag/AgCl having the constant potential +199 mV vs. normal hydrogen electrode.

The main parameters that affect the tribocorrosion process are: the type and range chosen for the normal forces applied, the contact frequency, the contact size (point, line, surface area), the vibrations, the environment (air, electrolytes, gases), and the materials used (compositional, surface roughness, crystallographic texture, residual stresses, etc.). In the case of unidirectional friction, in addition to adjusting the normal force applied, the rotation speed and the number of friction cycles can be adjusted. The resulting wear trace in the form of a circle can be studied ex-situ by electron microscopy methods for morphology or by micro topography methods to assess the loss of material due to both the corrosion process and the mechanical wear process. To set the bidirectional friction, in addition to adjusting the normal force, the friction frequency, the friction amplitude and the number of friction cycles can also be studied by microscopic and micro topographic methods.

The essential condition for carrying out tribo-corrosive experiments is therefore the possibility to control not only the mechanical conditions, but also the chemical-electrochemical test conditions. In aqueous ionic electrolytes, electrochemical techniques offer the possibility to control in situ and in real time the surface reactivity of metals and other electrically conductive materials. Therefore the material to be studied, as working electrode (WE) is mounted in an electrochemical cell connected to an electrochemical workstation [11].

Corundum balls or alumina pin are loaded on top of the tested material. For example, the results obtained for the tribocorrosion tests of 304L stainless steel compared to the Co/nano-CeO_2 nanocomposite layers – 30 g/L, in Hank biological solution [11] in the unidirectional continuous friction system, pin on disc, when a force of 5 N is applied a with a rotation rate of 120 rpm and a friction period of 5000 cycles.

For the second bidirectional, friction system the example refers to the untreated titanium alloy Ti6Al4V and the alloy subjected to controlled oxidation [9,17] to form a thin layer of nanoporous titanium oxide on its surface. The 400 mN normal force is applied at a sliding frequency of 5 Hz with 500 μm displacement amplitude and 1000 sliding cycles in Fusayama Meyer saliva solution.

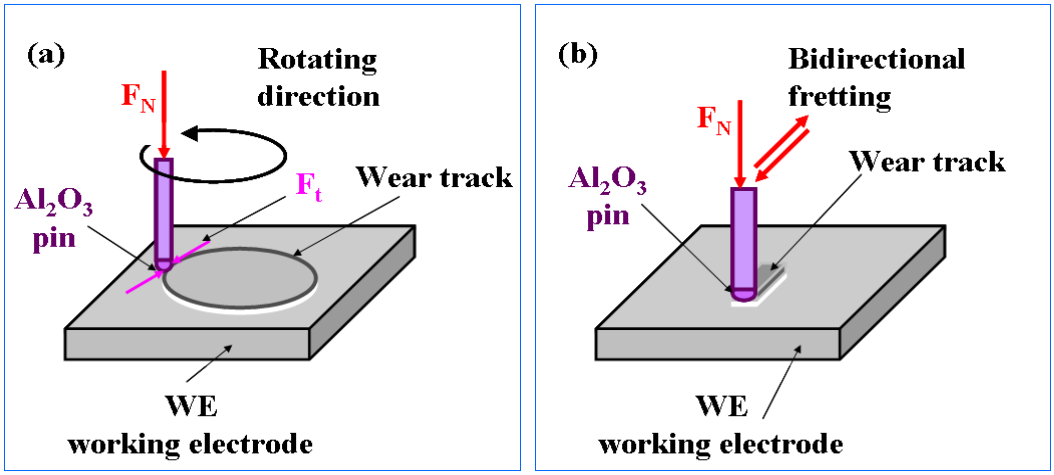

Fig. 1. Experimental set-up for tribocorrosion tests: (a) unidirectional pin on disc friction; (b) bidirectional fretting

Among the biomaterials tested in the degradation process by tribocorrosion are 304L stainless steel, nanocomposite layers or titanium alloys such as Ti6Al4V.

304L stainless steel is tested for tribocorrosion in Hank biological solution and with the same parameters as the Co/nano-CeO_2 nanocomposite layers obtained by electro-codeposition of CeO_2 nanoparticles with cobalt [11].

Stainless steel is a material that is often used in the biomedical field, especially in various structures in dentistry. Tribocorrosion aspects of 304L stainless steel in Ringer biological solution were studied by another way of sampling and another way of friction by bidirectional friction, with an amplitude of 200 µm [10,18].

Ti6Al4V is a well-known titanium alloy used in implantology [9,17,19-20] and some surface modification techniques are used in order to improve its properties [9,17,19-20].

The electrochemical measurements used are time measurement of free potential (OCP) and recording of electrochemical impedance spectroscopy before friction, during friction and after stopping friction.

3. Results and discussion

3.1. Open circuit potential (OCP)

Open circuit potential (OCP), also called equilibrium potential or corrosion potential, is the working electrode potential relative to the reference electrode when no potential or current is applied to the electrochemical cell. OCP is a mixed potential caused by oxidation and reduction reactions that take place on the surface of a metal electrode. The open circuit potential technique or the equilibrium potential monitoring technique is the simplest and most widely used method in measuring corrosion and tribocorrosion resistance.

Using a potentiostat and a reference electrode (RE), the OCP evolution of a working electrode (WE) can be monitored during immersion in an electrolyte. The potential is a basic indicator of the thermodynamic state of the material surface in relation to the electrolyte. Can be used in conjunction with Pourbaix diagrams. The OCP may provide information on the active or passive behavior of the investigated metallic material in a given system.

For example, the formation of the oxide film on the surface of a passive metal or alloy may become more protective over time, resulting in a change in potential in a nobler direction. In Fig. 2 it is shown the open circuit potential of 304L stainless steel and nanocomposite layer Co/nano-CeO_2 (30 g/L) recorded during immersion period in biological Hank solution. Both materials show a passive state of surface during all period of immersion (18 hours) before starting the friction.

On the contrary, a change in potential in a negative direction, more active, may indicate a loss of passivity. Moreover, the OCP recorded during tribocorrosion tests is a mixed potential that reflects the condition of the material in the worn area and of the material outside the track area [10,21-23]. Figure 3 shows the evolution of the free potential of 304L stainless steel and nanocomposite layer Co/nano-CeO_2 (30 g/L) for the tribocorrosion tests by applying a force of 5 N by continuous unidirectional fretting (pin-on-disc) in Hank biological solution. At immersion time, it was observed the open circuit potential value of each studied surface.

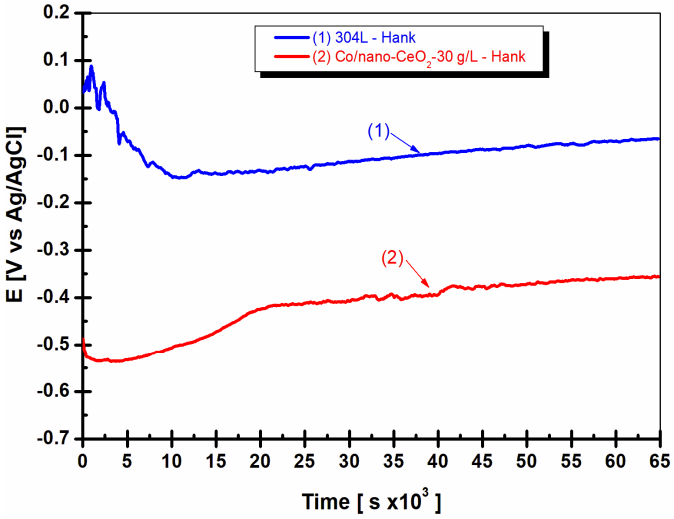

Fig. 2. Evolution of open circuit potential during immersion in Hank biological solution of: (1) 304L stainless steel; (2) Co/nano-CeO_2 (30 g/L) nanocomposite layer

In Fig. 3 the evolution of the free potential is observed when immersing the samples in the biological Hank solution, before applying the friction force (for a short time), during friction period and after stoping the force and stopping the friction.

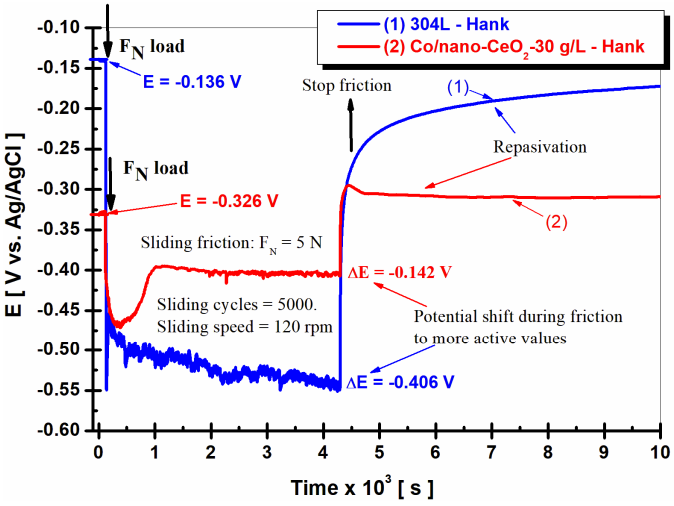

Fig. 3. Evolution of open circuit potential at immersion time in Hank biological solution, during friction by applying a normal force of 5N and after stopping the friction of: (1) 304L stainless steel; (2) Co/nano-CeO_2 (30 g/L) nanocomposite layer

The surface of 304L stainless steel show a passive state having a potential value of E = –0.136 V vs. Ag / AgCl, while Co/nano-CeO_2 nanocomposite layer show a steady state of

open circuit potential at more negative value of E = –0.326 V vs. Ag/AgCl.

Analyzing Fig. 3, it can be noticed that when applying the 5N force, the value of the open circuit potential suddenly decreases to –0.546 V vs. Ag / AgCl for 304L stainless steel, curve (1).

The shift of potential at starting the friction to more negative or active values is ΔE = –0.406 V. The value of the free potential during the friction tends to decrease slightly towards more negative values, so that at the friction stopping, this value is more negative reaching a value of –0.548 V vs. the reference electrode used. However, the potential difference during the friction period is less than 0.00167 V.

Also in the case of nanocomposite layers, it is observed that when the normal force is applied and friction begins, the surface of the nanocomposite layer is degraded. This degradation leads to a sudden decrease of the open circuit potential towards a more active cathodic direction at a value of E = 0.406 V vs. Ag/AgCl, which indicates the appearance of a corrosion process during the wear of the surface. The difference in the potential to decrease from the passive state to the active state when applying the 5N force is much smaller than in the case of 304L steel, being ΔE = 0.142 V. During friction period, the potential tends to be constant.

The decrease of the potential towards more negative values is smaller for the nanocomposite layers due to the CeO_2 nanoparticles incorporated in the cobalt matrix, which ennobles their electrochemical behavior and, therefore, increases their resistance to the wear-corrosion process [11].

This behavior indicates that when the 5 N normal force is applied, the wear track is more difficult to repassivates, the degradation of the steel surface following the wear being more pronounced compared to the Co/nano-CeO_2 nanocomposite layer immersed in the Hank solution at the applied 5 N load.

After stopping the friction force, the free potential suddenly moves to more positive values, reaching the value of E = –0.1836 V for 304L stainless steel, which is with 0.04396 V more negative than the free potential value of the passive stainless steel before the application of the friction force 5 N. This behavior confirms both the capacity of repassivation of the steel surface in the area of the wear track but also a greater degradation in the area of the wear track that can no longer return to its initial state, after friction with 5 N in Hank biological solution.

After the end of the wear tests when the friction is stopped, it is observed also that the OCP values for nanocomposite layer have increased suddenly, because the surface is repassivated, the passive value of the open circuit potential being more positive, E = –0.3 V vs. Ag/AgCl, that the value recorded before starting the friction. These increasing values of OCP is more positive for nanocomposite layers, due to a mixed oxide consisting of cobalt oxide and cerium oxide on their surface [11].

As it can be seen in Fig. 3, the highest potential shift to more active values at the application of the 5 N friction force is recorded for 304L stainless steel, E = 0.406 V, which confirms that it is most sensitive to the degradation by friction in a corrosive environment, ie, the most sensitive to degradation by tribocorrosion (simultaneous corrosion and wear). In addition, 304L stainless steel can no longer reach the initial value of the passive potential recorded before friction, confirming the irreversible changes on its surface degradation under these fretting conditions.

The least affected by the tribocorrosive degradation process is the nanocomposite Co/nano-CeO_2 (30 g/L), whose potential at the start of the friction force of 5 N moves to more negative (active) values only with E = 0.1425 V. In addition, the repassivation potential of the nanocomposite surface, after stopping the friction force, reaches even more positive (noble) values than the initial value recorded before starting the friction force.

We can say that friction highlights several CeO_2 nanoparticles on the surface of the nanocomposite, which further gives it a better resistance to the tribocorrosive degradation process, as will be highlighted further by the analysis of friction tracks [11].

In Fig. 4 is shown the open circuit potential of Ti6Al4V alloy untreated and oxidized layer by applying a corundum balls loaded on the top of the samples at normal force of 400 mN, sliding frequency of 5 Hz, 500 μm displacement amplitude and 1000 sliding cycles [19-20].

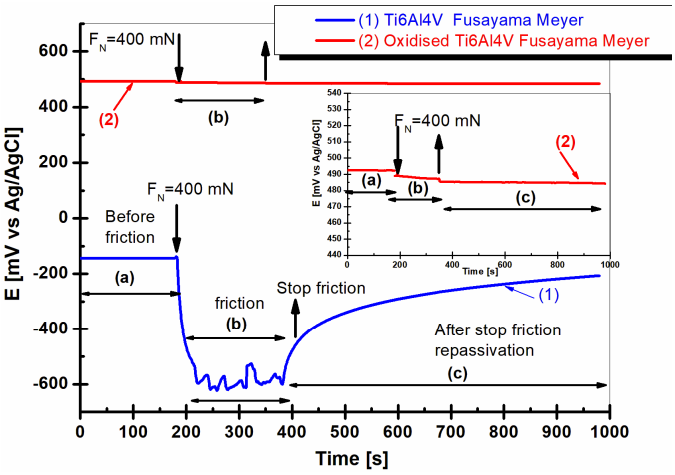

Fig. 4. Open circuit potential versus time time plots obtained in Fusayama – Meyer saliva just before (a), during friction (b) and after friction force is stopped (c) for: (1) untreated Ti-6Al-4V alloy surface, (2) anodic nanoporous TiO_2 surface

A zoom for OCP evolution of oxidized Ti6Al4V alloy was inserted inside of Fig. 4 in order to see better the very small shift of open circuit potential when the friction starts. It is well observed the lower effect of the friction force on the surface of the oxidized titanium alloy.

The untreated Ti6Al4V alloy is in a passive state before friction start, Fig. 4 (1) zone (a), having an open circuit potential value of E = –143 mV vs. Ag/AgCl.

When applying the friction force, the potential suddenly shifts to more negative values, E = –591 mV vs. Ag/AgCl, being approximately constant during friction, Fig. 4 (1) zone (b). The potential difference between the passivation state and the active state during friction is 449 mV.

When the friction is stopped, the alloy surface repassivates, Fig. 4 (1) zone (c), but the potential fails to reach the initial value before friction, reaching only a value of $E = -217$ mV vs. Ag/AgCl. This behavior suggests an irreversible degradation of the alloy surface that will be reflected in the deficient behavior of the respective implant subjected to both the biological corrosive environment and the specific movement of the implant site.

On the oxidized surface of the titanium alloy there is a better state of passivity given by the oxide layer formed controlled on its surface, the free potential being $E = 493$ mV vs. Ag/AgCl, Fig. 4 (2) zone (a). When the same friction force is applied, the shift of the free potential towards more active values is very small, reaching only the value $E = 487$ mV vs. Ag/AgCl, Fig. 4 (2) zone (b). The potential difference between the passive state and the active state during friction is very small being only 0.006 mV, Fig. 4 (2) zone (b). After stopping the friction, the oxidized surface of the titanium alloy remains in a passive state with a free potential of $E = 485$ mV vs. Ag/AgCl, Fig. 4 (2) zone (c). This behavior suggests that the controlled oxide layer formed on the surface of the titanium alloy does not deteriorate during the tribocorrosion process, which will have a beneficial effect on the implant.

3.2. Electrochemical impedance spectroscopy (EIS)

Electrochemical impedance spectroscopy (EIS) is the most sophisticated technique among the electrochemical methods in this study being imposed to characterize the reactivity and polarization resistance of different materials in specific application solutions. For EIS measurements, a 10 mV sinusoidal signal variation is imposed versus open circuit potential at frequencies from 10^4 Hz to 10^{-3} Hz, 10-20 frequencies per decade, recorded before the friction tests, during the friction and after the friction is stopped, at different applied loads.

In the tribocorrosion tests of 304L stainless steel and Co/nano-CeO_2 nanocomposite layer the rotational rate is chosen at 120 rpm and the total number of cycles for each test is set at 5000 cycles.

The recorded electrochemical impedance results recorded before friction in the passive state, during friction in the active state and after friction is topped in the repassivation state are shown in Figs. 5 and 6.

Nyquist diagram, Fig. 5 shows the imaginary part of the impedance, –Im Z, compared to the real part, Real Z, represented as a arc of a circle. To simulate the experimental data, the Zview program (Scribner Associates Inc.) can be used, and the quality of the experimental and fitted data is evaluated using the deviation of the chi-square mean value, which in this study has the values less than 10^{-3}. For the simulation of the experimental data a simple equivalent electrical circuit composed of (R_s, CPE, R_p) [11,24-25] can be used where R_s is the resistance of the solution (represents the resistance of the solution between the reference electrode and the working electrode).

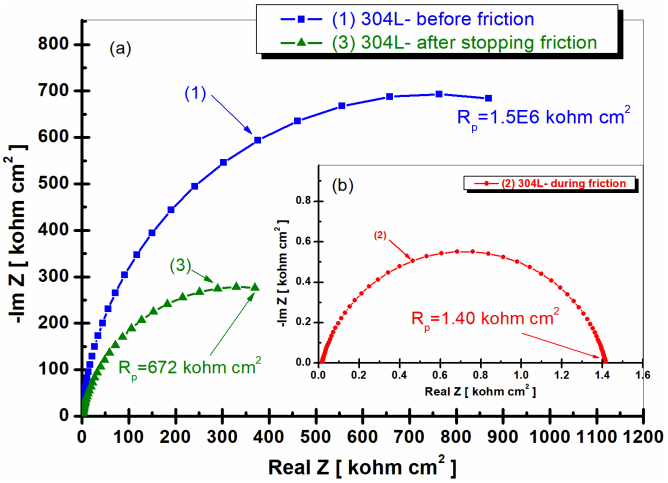

Fig. 5. Nyquist representation of electrochemical impedance spectroscopy diagrams of 304L steel immersed in Hank's solution: Layer (a) – (1) before friction; Layer (b) – (2) during friction after the application of the normal force of 5N; Layer (a) – (3) after stopping the friction and repassivation of surface

R_p represents the polarization resistance of 304L stainless steel, which is the transition resistance between electrodes and electrolyte. The polarization of an electrode causes the current to flow due to electrochemical reactions at the electrode surface. High R_p value for 304L stainless steel before friction, Fig. 5 (1) indicates a high corrosion resistance at the electrode surface. CPE is a constant phase element, which is used instead of the capacity of the electric double layer, C_{dl}, to simulate impedance data whose Nyquist diagram is not a perfect semicircle and may be due to the uneven and inhomogeneous electrode surface, roughness, or other effects structural. The impedance of such an electrochemical system with CPE is expressed by Eq. (1) [11,25].

$$Z_{CPE} = \frac{1}{Q(j\omega)^{\alpha}} \tag{1}$$

Where Q is the real frequency-independent constant, CPE is expressed in $F\ cm^{-2}$, ω the angular frequency ($2\pi f$) in rad s^{-1}, f is the frequency in Hz, j is the imaginary number, $j = \sqrt{-1}$, α is the angle of rotation of the capacitive lines on the complex plane. The parameter α can take values from –1 to 1.

Figure 5 (2), layer (b) shows a large decrease of the polarization resistance of the stainless steel surface during friction by several orders of magnitude (about 1000), at $R_p = 1.40$ kohm·cm^2, compared to the polarization resistance recorded before friction, with the value of 1500 kohm·cm^2. This drastic decrease in corrosion resistance during friction demonstrates that the surface of the stainless steel is active during friction and is subject to electrochemical corrosion in the Hank solution. Therefore, in this case for the equivalent electrical circuit it is more correct to use the charge transfer resistance, R_{ct}, instead of the polarization resistance, R_p. The predominant phenomenon during friction is the degradation of stainless steel both due to the friction and destruction of the passive film after wear and the corrosive dissolution of the material after wear after the break of the passive film, so tribocorrosive wear. From Fig. 5 (3) it can also be

seen that after stopping the friction the surface of the stainless steel repassivates, the polarization resistance is increasing to 672 kohm·cm^2, without reaching the initial value showed for the passive state, confirming as in the case of measuring free potential, that the surface of 304L stainless steel suffers an irreversible degradation during friction.

The complex plane representations (Nyquist) of the EIS results before friction, during friction and after stopping the friction force for the Co/nano-CeO_2 nanocomposite layer are shown in Fig. 6.

In Fig. 6, layer (a) curves (1), the Nyquist diagram for the Co/nano-CeO_2 layer before friction is shown. In Fig. 6, layer (b), curve (2) it is shown the Nyquist diagram of the EIS results for the same system obtained during friction with a normal load of 5 N, while in Fig. 6, layer (a) curves (3) is represented the Nyquist diagram of the EIS results for the same nanocomposite layer after the friction force and therefore the frictional wear have been stopped.

From Fig. 6, layer (a) curve (1) it is observed that before the friction tests the polarization resistance, R_p, for the Co/nano-CeO_2 layer studied, reaches the value of R_p = 12.230 kohm·cm^2.

With the application of the friction force of 5 N, Fig. 6, layer (b) curve (3) we notice that the R_p value suddenly decreases by approximately three times as compared to the value obtained from the EIS in the absence of disturbing factors, R_p = 3.312 kohm·cm^2.

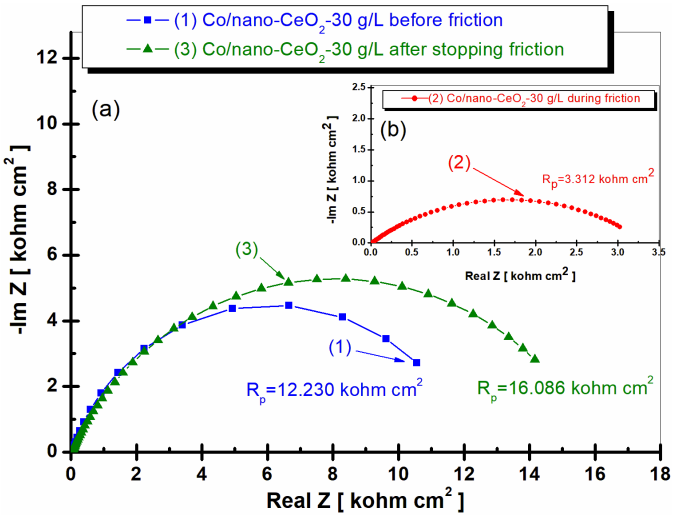

Fig. 6. Nyquist representation of electrochemical impedance spectroscopy diagrams of nanocomposite layer Co/nano-CeO_2 30 g/L immersed in Hank's solution: Layer (a) – (1) before friction; Layer (b) – (2) during friction after the application of the normal force of 5N; Layer (a) – (3) after stopping rubbing

The slight decrease in polarization resistance value during friction in the case of the Co/nano-CeO_2 nanocomposite layer, compared to 304L stainless steel can be explained by the beneficial effect of the nano-CeO_2 nanoparticles incorporated into the cobalt matrix, which induce an increase in microhardness and therefore a higher resistance to mechanical disturbance caused by friction.

After the end of the friction tests, we also notice that for the studied nanocomposite layer, the R_p value increases more than the one measured before friction, R_p = 16.086 kohm·cm^2.

In Figs. 7 and 8 there are shown the electrochemical impedance spectroscopy results recorded for Ti6Al4V alloy and oxidised Ti6Al4V alloy in Fusayama Meyer solution before friction, during bidirectional friction with an applied normal force of 400 mN and after the friction force was stopped.

The EIS spectra in the complex plane (Nyquist) revealed incomplete semicircles, with a very large radius of curvature, which shows a capacitive behavior, suggesting a protective layer, passive, very resistant.

In this case, the equivalent circuit models used to simulate the electrochemical impedance data for the two types of surfaces studied consider a circuit for bulk titanium alloy, which have a native very thin oxide layer and a circuit for the nanoporous titanium oxide formed electrochemically on its surface [9]. In these models, R_s represents the resistance associated with the electrolyte solution, R_c and Q_c are the resistance and the constant phase element (*CPE*-capacitive characterization of the electric double layer at the sample-electrolyte interface) associated with the compact native oxide layer, which forms spontaneously on titanium alloys, R_p and Q_p the resistance and the constant phase element associated with the porous oxide layer.

During immersion in Fusayama Meyer saliva solution Ti-6Al-4V alloy surface exhibit a higher polarization resistance, R_p value of 1430 kohm·cm^2, Fig. 7, curve (1).

Under fretting conditions, Fig. 7 curve (3), the untreated Ti-6Al-4V alloy surface has exposed a smaller value of R_p equal to 39 kohm·cm^2, being more than 1000 times smaller as it was under immersion conditions, before friction. This is due to the removal of the passive film in the friction zone (wear track) under sliding conditions, suggesting the detrimental influence of sliding action on untreated alloy surface immersed in saliva solution, which will be reflected in poor behavior of further implant.

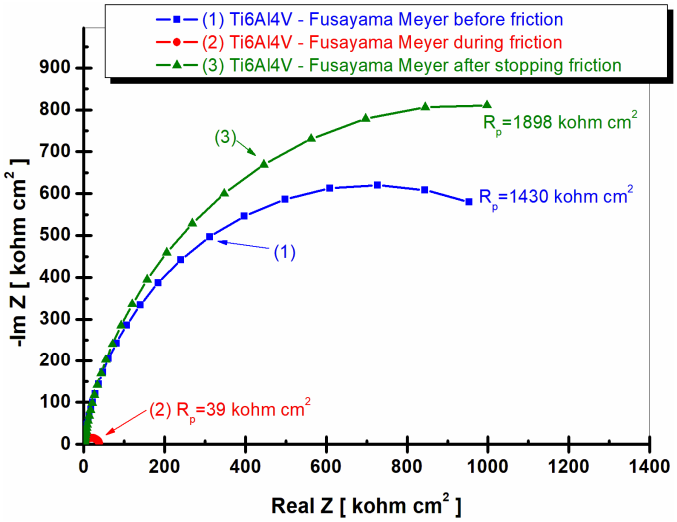

Fig. 7. Nyquist representation of electrochemical impedance spectroscopy diagrams of Ti6Al4V alloy immersed in Fusayama Meyer solution: (1) before friction; (2) during friction after the application of the normal force of 400 mN; (3) after stopping the friction force

After the friction is stopped, Fig. 7 curve (3), the electrochemical impedance spectroscopy of untreated Ti6Al4V alloy repassivates showing a little higher specific resistance which still remains in the same order of magnitude, R_p = 1898 kohm·cm^2.

In the case of the surface of the anodic oxidized Ti6Al4V alloy, the electrochemical impedance spectroscopy diagrams are shown in Fig. 8, curves (1), (2) and (3).

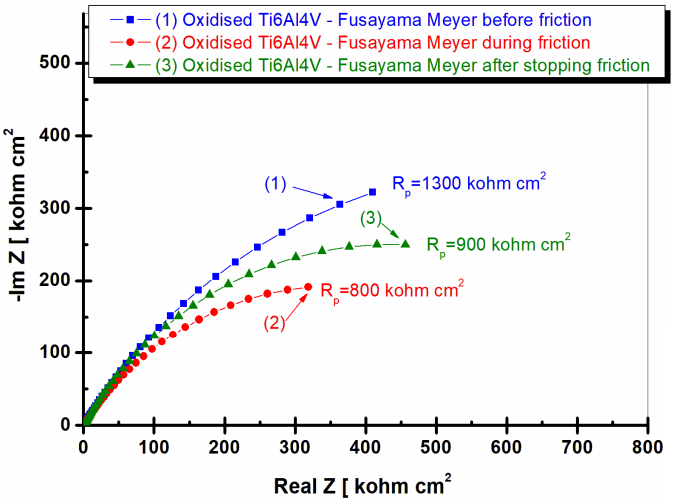

Fig. 8. Nyquist representation of electrochemical impedance spectroscopy diagrams of oxidised Ti6Al4V alloy immersed in Fusayama Meyer solution: (1) before friction; (2) during friction after the application of the normal force of 400 mN; (3) after stopping the friction force

It is found that the specific resistance recorded after friction and during friction did not change too much as compared to the specific resistance before the friction force is loaded. Thus the specific polarization resistance before friction has a value of R_p = 1300 kohm·cm^2, Fig. 8, curve (1), decreasing only to R_p = 800 kohm·cm^2 during friction, Fig. 8 curve (2) and returning to a value close to the value before friction, R_p = 900 kohm·cm^2, Fig. 8, curve (3).

If we look carefully to the electrochemical impedance spectroscopy diagrams recorded during friction for untreated Ti6Al4V alloy, Fig. 7, curve (2) and for electrochemically oxidized Ti6Al4V alloy, Fig. 8, curve (2) it is very clear that the modification of the surface of the titanium alloy greatly improves its resistance to degradation by tribocorrosion. Thus the specific polarization resistance of the untreated titanium alloy recorded during friction is only 39 kohm·cm^2 while the specific polarization resistance of the oxidized alloy with the nanoporous layer of titanium oxide is ten times higher, having the value of 800 kohm·cm^2.

4. Conclusions

This work reflects the importance of electrochemical techniques to study the degradation of biomaterials by tribocorrosion process (wear and corrosion) in specific biological fluids.

Electrochemical measurements, such as free potential and electrochemical impedance spectroscopy, performed during tribocorrosion tests make it possible to obtain in situ information about the surface conditions of the biomaterial subjected to friction and corrosion in specific environement.

Electrochemical measurements performed during tribocorrosion tests show that the oxidation kinetics and mechanical fractures of the passive film on the surface must be taken into account. The area of the active surface subject to friction must be provided as a dynamic quantity, which evolves continuously or cyclically during the tests.

The open circuit potential technique used in measuring the tribocorrosion process provide information on the active or passive behavior of the investigated metallic biomaterial in the biological fluid, before, during friction and after stopping the friction.

The electrochemical impedance spectroscopy measurements clearly indicate that the passivation and depassivation process occurs on the area subject to friction of the biomaterial immersed in the biological solution, and bring valuable information about the state of restoration of the passive film on the rubbed area.

Acknowledgements

All the experimental work was performed at Competences Center Interfaces – Tribocorrosion and Electrochemical Systems (CC-ITES). The authors would like to express appreciation for Prof. Jean-Pierre Celis from Katholieke University of Leuven, Belgium and Prof. Pierre Ponthiaux from Ecole Centrale Paris, France for they valuable scientific advice.

REFERENCES

[1] P. Ponthiaux, F. Wenger, D. Drees, J.P. Celis, Wear **256**, 459-468 (2004).
[2] I. García, D. Drees, J.P. Celis, Wear **249**, 452-460 (2001).
[3] J. Rituerto Sin, S. Suñer, A. Neville, N. Emami, Tribol. Int. **75**, 10-15 (2014).
[4] L. Benea, P. Ponthiaux, F. Wenger, J. Galland, D. Hertz, J.Y. Malo, Wear **256** (9-10), 948-953 (2004).
[5] P. Ren, H. Meng, Q. Xia, Z. Zhu, M. He, Corros. Sci. **180**, 109185 (2021).
[6] D. Landolt, S. Mischler, M. Stemp, Electrochim. Acta **46**, 3913-3929 (2001).
[7] L. Benea, S.B. Bașa, E. Dănăilă, N. Caron, O. Raquet, P. Ponthiaux, J.P. Celis, Mater. Design **65**, 550-558 (2015).
[8] L. Benea, N. Caron, O. Raquet, RSC Adv. **6**, 59775-59783 (2016).
[9] L. Benea. E. Danaila, P. Ponthiaux, Corros. Sci. **91**, 262-271 (2015).
[10] A. Berradja, F. Bratu, L. Benea, G. Willems and J.P. Celis, Wear **261** (9), 987-993 (2006).
[11] L. Benea, N. Simionescu, J.P. Celis, J. Mech. Behav. Biomed. Mater. **101**, 103443 (2020).
[12] M.T. Mathew, J.J. Jacobs, M.A. Wimmer, Clin. Orthop. Relat. Res. **470** (11), 3109-3117 (2012).

[13] M.T. Mathew, M.A. Wimmer, 13 – Tribocorrosion in artificial joints: in vitro testing and clinical implications, Bio-Tribocorrosion in Biomaterials and Medical Implants, Woodhead Publishing, Sawston (2013).

[14] C. Dini, R.C. Costa, C. Sukotjo, T.G. Christos, M.T. Mathew, A.R.V. Barão, Front. Mech. Eng. **6**, 1 (2020).

[15] N. Eliaz, Degradation of implant materials, Springer, New York (2012).

[16] S.A. Alves, A.L. Rossi, A.R. Ribeiro, F. Toptan, A.M. Pinto, J.P. Celis, T. Shokuhfar, L.A. Rocha, Wear **384-385**, 28-42 (2017).

[17] L. Benea, E. Mardare-Danaila, J.P. Celis, Tribol. Int. **78**, 168-175 (2014).

[18] F. Bratu, L. Benea, J.P. Celis, Rev. Chim. (Bucuresti), **59** (3), 346-350 (2008).

[19] L. Benea, Studying tribocorrosion processes in biomedical and industrial applications, CD Proceedings Volume of 8th International Conference on Tribology – Balkantrib'14, 30 October – 1 November 2014, Sinaia, Romania, 425-431. ISBN: 978-973-719-570-8.

[20] E. Dănăilă, L. Benea, J.P. Celis, Tribo-electrochemical characterization of Ti-6Al-4V alloy and nanoporous TiO_2 layer in simulated body fluid solution, CD Proceedings Volume of 8th International Conference on Tribology – Balkantrib'14, 30 October – 1 November 2014, Sinaia, Romania, 455-458. ISBN: 978-973-719-570-8.

[21] A. López-Ortega, J.L. Arana, R. Bayón, Int. J. Corros. 7345346, 1-24 (2018). DOI: https://doi.org/10.1155/2018/7345346

[22] J. Géringer, B. Boyer, K. Kim. Fretting corrosion in biomedical implants. D. Landolt, S. Mischler, Tribocorrosion of passive metals and coatings, Woodhead Publishing Limited (2011). https://hal.archives-ouvertes.fr/hal-00683150

[23] P. Ponthiaux, F. Wenger, and J.P. Celis, Tribocorrosion: Material Behavior Under Combined Conditions of Corrosion and Mechanical Loading, Corrosion Resistance, In Tech, ISBN: 978-953-51-0467-4 (2012). DOI: http://dx.doi.org/10.5772/35634

[24] N. Diomidis, J.P. Celis, P. Ponthiaux, F. Wenger, Wear **269** (1-2), 93-103 (2010).

[25] A. Lasia, Electrochemical Impedance Spectroscopy and its Applications, in: B.E. Conway, J.O.M. Bockris, R. White (Eds.) Modern Aspects of Electrochemistry, Springer, US (2002).